Saturation-specific pattern of acquired colour vision deficiency in two clinical populations revealed by the method of triads

David L. BIMLER[1], Galina V. PARAMEI[2], Claudia FEITOSA-SANTANA[3], Nestor Norio OIWA[4] & Dora Fix VENTURA[5]

[1]School of Arts, Development and Health Education, Massey University College of Education, Palmerston North, New Zealand
[2]Department of Psychology, Liverpool Hope University, Liverpool, United Kingdom
[3]Department of Psychology, Chicago State University, Chicago, USA
[4]Department of Biomedical Sciences, Universidade Federal Fluminense, Nova Friburgo, Brazil
[5]Núcleo de Neurociências e Comportamento & Departamento de Psicologia Experimental, Instituto de Psicologia, Universidade de São Paulo, São Paulo, Brazil

Corresponding author:
David L. Bimler
School of Arts, Development and Health Education
Massey University College of Education
Palmerston North, New Zealand
E-mail: dbimler@massey.ac.nz

Running Head: Method of triads reveals saturation-specific colour vision deficiency in clinical populations

Keywords: colour vision deficiencies; colour spaces; D-15; D-15d; diabetes mellitus type 2; mercury exposure; method of triads; multidimensional scaling; Maximum Likelihood; individual differences

Abstract

Subjective colour spaces were reconstructed for persons occupationally exposed to mercury (Hg) and patients with diabetes mellitus type 2 (DM-2), two groups at risk for acquired colour-vision deficiency, and compared with healthy normal trichromats. Judgments of colour dissimilarity were collected with the method of triads, applied to a composite assortment of colour samples. These were drawn from two widely-used colour arrangement tests – ten hues from the Farnsworth D-15 test and five from the Lanthony Desaturated D-15d test, ensuring that the assortment sampled two levels of lightness and saturation. The data were analysed with Maximum-Likelihood multidimensional scaling (MDS) and within a novel Individual-Differences MDS model to estimate subject-specific parameters. The MDS solutions for the two clinical groups showed a compression along a Blue-Yellow axis, limited however to desaturated hues. This result was confirmed by the individual-differences model. In addition, the clinical groups were found to place significantly higher weights on the lightness differences between stimuli, conceivably to compensate for their reduced chromatic discrimination. The specific form of colour-space distortion in the clinical groups indicated an increase in their thresholds for blue-yellow signals, providing insights into the nature of impairment mechanisms. The results have implications for stimuli and diagnostic procedures for testing individual differences in color vision, and for analyzing the responses. The present approach is sensitive to distinctive patterns of subtle colour-vision impairment underestimated by the conventional D-15d test.

Introduction

The D-15 and D-15d are two widely-used tests for detecting and quantifying deficits of colour perception.[1,2] Both are 'panel tests' in which 16 coloured samples, located by their specifications in colour space so as to form an incomplete circle, must be arranged into the correct rainbow sequence. In each case an error score measures overall loss of colour discrimination. These tests also qualify the *nature of* colour vision loss, distinguishing blue-yellow (B/Y) and/or red-green (R/G) impairment. Their advantages include speed and convenience; the D-15d, in addition, is sensitive to mild forms of colour vision impairment. The D-15 is designed for classifying an individual within the diagnostic taxonomy of *congenital* colour vision deficits, determining the 'polarity' of the deficiency, i.e. B/Y or R/G, if it exceeds a threshold of severity. The D-15d lends itself well to assessing *acquired* deficits where early detection of a progressive impairment can be crucial, and is less clear-cut, i.e. the breakdown by polarity is often less clear than for congenital deficiency. For these reasons, the D-15d sees applications in many clinical studies [3-5] as well as in the area of occupational optometry, where deficits may be the result of work-related exposure to toxins (for a review see Ref. 6).

From one perspective, a subject's responses to panel tests such as the D-15 and D-15d can be regarded as a ranking of the pairwise dissimilarities among the colour samples, from most-similar to the least-similar pair.[7] A subject may approach the samples with some alternative procedure – sorting them into groups, for instance – and as long as the responses can be treated as comparisons amongst dissimilarities, they can be analysed within the same over-arching framework.

Bimler and Kirkland [8] used the method of triads [9] to elicit 'odd-one-out' data for a combined set of D-15 and D-15d samples, presenting a series of triadic combinations to each subject who had to choose the least similar sample from each three. Most combinations require saturated, darker stimuli from the D-15 to be considered against desaturated, lighter ones from

the D-15d, so the odd-one-out choice may vary if the observer places more weight on either hue or lightness differences. In addition, a triad might probe similarities at the scale of barely-discernable differences (as with the D-15d) or at a coarse, supra-threshold scale (with D-15), depending on its constituent samples. Analysis of the data with multidimensional scaling (MDS) allows a subjective colour space to be reconstructed for each individual or certain groups of individuals.[10] This analysis of similarity data from the combined colour samples has revealed subtle differences, for example, between smoking and non-smoking groups,[11] monozygotic and dizygotic twins,[12] between females and males [8] and between homozygous females and heterozygous carriers of colour vision deficiency.[13]

For clinical populations, Feitosa-Santana and her colleagues elicited odd-one-out responses of this form – for randomized triads of a combined D-15 and D-15d stimulus set – for age-matched normal controls and groups whose colour vision had potentially been impaired by exposure to mercury vapour[14] or by diabetes mellitus type 2.[15] For convenience, though without losing generality or statistical power, the triads in these studies did not follow a predetermined list, but rather were generated randomly.

The MDS solutions for both clinical groups[14,15] revealed distributions significantly different from those in the respective control groups. The clinical groups' colour spaces tended to show a greater level of distortion and higher variability in the locations of stimuli along the B/Y axis, i.e. possible tritan-type polar deficiency with a B/Y confusion axis.

In the present study we are interested in whether the variations between individuals – and between clinical and control groups – take the form of relative insensitivity along specific directions in colour space, since a specific loss of sensitivity can provide clues to the neural locus (or loci) of the visual system implicated in an acquired deficiency. As Krastel and Moreland (Ref. 16, p. 117) note, "…acquired tritan deficits may be subjectively quite unobtrusive and well tolerated"; that is, decreases in hue discrimination (i.e. increased thresholds) do not necessarily affect subjective colour experience or reach the level of

awareness. The method used here allows for the possibility of capturing subtle hue discrimination impairments by using relatively desaturated stimuli along with saturated ones. Thus subjects are required to consider small hue differences (close to threshold) between relatively similar pairs of stimuli, as well as larger, supra-threshold differences.

In the geometrical paradigm, a polar deficiency is represented as a *compression* of colour space.[10] Here this was tested by re-analysing the data of Feitosa-Santana et al.[14,15] within the framework of individual-differences MDS. The latter imposes a single geometrical solution upon all the subjects, while allowing that solution to vary in a particular way (compression along a confusion axis) controlled by a small number of parameters, to fit it to each subject's responses. A subject's data are thereby boiled down to their values of the parameters.

Acquired colour vision impairment and occupational mercury exposure

Mercury, both in its elemental form (e.g. mercury vapour) and as an organic compound (methylmercury), is a potent neurotoxin that can cause a range of perceptual, motor and cognitive impairments.[17-20]

Inter alia, mercury exposure is known to affect colour vision.[21-23] The impairment manifests itself, in particular, as increased colour discrimination thresholds and decreased chromatic contrast sensitivity.[24,25] As Pokorny, Smith, Verriest, and Pinckers (Ref. 26, p. 309) note , "[a] generalized depression of optic nerve conduction characterized by peripheral constriction of the visual fields and optic atrophy is a clinical picture found in […] mercury toxicity (Minimata disease)". In the periphery of the visual system, impairment of inner and outer retinal function was found, indicating damage to post-receptoral structures.[25] Nor can damage to the visual cortex be excluded.[27,28] Estimating specific loss of sensitivity, i.e. delineation of the confusion axes in colour space, can provide clues to the neural locus (or loci) affected by mercury.

The D-15d test revealed higher error scores in mercury exposed persons, with a higher frequency of blue-yellow confusion [Type III dyschromatopsia, according to Verriest's classification[29]], regardless of whether they were exposed occupationally[21,23] or via contaminated food.[18,19] Employment of the Farnsworth-Munsell 100-hue test (FM-100) showed that mercury-contaminated subjects performed significantly worse than matched controls, but revealed no distinct confusion axis in colour space.[24]

When tested with the Cambridge Colour Test (CCT),[30] subjects exposed to mercury revealed increased chromatic discrimination thresholds along all three confusion axes (protan, deutan and tritan) and non-selective enlargement of MacAdam ellipses. These findings related to gold miners,[24] workers in the fluorescent-tube industry (Feitosa-Santana et al., 2008)[25,28,31] and dentists, exposed through dental amalgam.[32]

Development of colour vision impairment in diabetes mellitus type 2

The sequelae of diabetes mellitus include colour vision impairment: persistent hyperglycemia causes retinal micro vascular changes that damage the retina (diabetic retinopathy, DR), leading to losses in visual acuity and contrast sensitivity, as well as in colour vision.[33] In diabetic patients, elevated thresholds for cone photoreceptors have been reported and attributed to the concentration of circulating glucose and a reduction of the oxygen supply.[34] Notably, subclinical or mild colour vision impairment may precede DR to emerge at early stages of type 2 diabetes mellitus (DM-2), before the appearance of vascular alterations.

Colour vision of DM-2 patients was examined in many studies using panel tests, such as the FM-100, [35-37] as well as D-15 and/or D-15d test.[15,38] Anomaloscopy has been employed to estimate Rayleigh and Moreland matches for the two perceptual systems, R/G and B/Y respectively.[39] Crucially, the extrapolation from anomaloscope matching range to colour impairment is far from direct. More recently, the CCT has been used to estimate colour

discrimination thresholds along the protan, deutan and tritan confusion lines.[38]

An effect on the B/Y, or tritan system, is repeatedly found in DM-2 patients. In patients without DR, predominantly tritan losses were diagnosed,[33] however diffuse losses were reported as well.[40,41] In DM-2 patients who had developed DR, losses in the B/Y system were found to increase with severity of DR.[33,42-44]

Feitosa-Santana et al. assessed colour vision impairment in DM-2 patients without diabetic retinopathy.[15,38] The present study re-examines those data.

Method

Subjects

All patients and controls underwent an ophthalmological examination, with the following inclusion criteria: best corrected Snellen visual acuity (VA) 20/30 or better; absence of retinopathy, ocular disease and posterior sub capsular cataract; maximum of grade 1 for cortical opacity (C1), nuclear colour (NC1) and nuclear opalescence (NO1) following the lens opacity classification system III (LOCS III). Clinical histories were collected to exclude alcoholism, smoking and systemic diseases that could affect the visual system. Observers with congenital colour deficiency were excluded using the D-15 test.

The mercury (Hg)-exposed group included 22 subjects who had been exposed to Hg vapour for at least five years working in fluorescent lamp industries. All had been discharged from work at least one year earlier and placed on disability retirement due to medical diagnosis of Hg intoxication based on clinical and laboratory examination. They had been referred by the Occupational Health Service of the Oscar Freire Institute of the University of São Paulo (Brazil). Table 1 in Ref. 14 tabulates details for 18 of these subjects (13 males), aged 42.1 ± 6.5 years; the four additional subjects had similar demographic characteristics.

The DM-2 group consisted of 32 patients (18 males), aged 30 to 76 years (50.5 ± 10.7), with disease duration from 0.5 to 27 years (9 ± 8.6). The absence of retinopathy was verified by fundoscopy (in 100% of the eyes) and by fundus photography and fluorescein angiography (62% of the eyes were examined; 100% of these lacked any sign of retinopathy).[31,38]

Twenty-three observers (15 males), aged 35 to 80 years (51 ± 12), served as controls. An age-matched subset of 18 of these observers were used as controls in Ref. 14 (Table 2), and 20 as controls in Ref. 15; age-matching was less rigid in the present analysis.

Procedure

The D-15 and D-15d tests each consist of 16 colour samples (plastic caps holding 12-mm circles of pigment on paper), occupying an incomplete circle in colour space. In Munsell denotation, the D-15 caps have Value = 5 and Chroma = 4;[1] the D-15d caps have the same hues but are lighter, with Value = 8, and less saturated, Chroma = 2.[2] Because of the lower saturation of the D-15d stimuli, differences between them are closer to threshold.[3,4,45] A composite assortment of 15 caps was created from the D-15 series by replacing caps No. 3, 6, 9, 12 and 15 with their counterparts from the D-15d and excluding the "pilot" caps, which were anchored to the test trays. This assortment was shuffled into five randomized groups of three. The subject viewed each triad in turn and chose the most dissimilar cap of the three (the odd-one-out).

No time limit was set. This procedure was repeated 12 times. The subject also judged five random triads created by shuffling the D-15 caps and five from the D-15d caps, providing a total of 70 triad judgments.[11,12] At the beginning of the session, the D-15 and D-15d caps were both used in the traditional way: the subject arranged them in a colour sequence, starting with the pilot cap and following each cap with the cap most similar to it.

The procedure was conducted monocularly. Control subjects were tested in only one eye. Subjects from the clinical groups repeated the procedure for both eyes (with random choice of testing left or right eye first) since acquired colour discrimination loss is not necessarily symmetrical.[29] Thus the 15 caps comprising the composite assortment were viewed 13 times by each control subject and 26 times by each clinical subject. The ten D-15d and five D-15 caps were viewed once by each control subject (in the five desaturated-only and five saturated-only triads respectively) and twice by each clinical subject.

Illumination of 500 lux was provided by two fluorescent lamps (Sylvania Octron 6500 K FO32W / 65K), with Coordinated Color Temperature = 6500K, Color Rendering Index = 75).

MDS analysis

We set out to reconstruct multidimensional colour spaces in which points represent the hues and are located so that the spatial distance between any two points reflects the perceived dissimilarity between that pair of hues. Each triad of caps corresponds to a triangle of points, in which the apex should be the hue chosen as odd-one-out.

For an initial exploratory analysis, the subjects' data were combined within each group and analysed with the existing 'MTRIAD' software[11-14] to obtain three separate solutions, i.e. consensus colour spaces for the controls, Hg and DM-2 groups. MTRIAD applies a maximum-likelihood algorithm, similar to the MAXSCAL algorithm for dissimilarity comparisons.[46] A Likelihood function $LL(\mathbf{X})$ quantifies the agreement between the solution and the individual triads comprising the data. $LL(\mathbf{X})$ is maximised in an iterative process that begins with initial estimates of the coordinates locating 30 points in the space, then adjusts them to progressively converge on a solution in which the inter-point distances are more likely than any other combination of distances to have produced the observed odd-one-out decisions. Appendix A

provides more detail (see also Ref. 7). A similar logic, in one dimension, features in Maximum likelihood difference scaling.[47,48] MTRIAD is available from the corresponding author.

To foreshadow the Results: constrained three-dimensional solutions were chosen for each group since we found that three dimensions provided a substantial improvement in Likelihood compared to two dimensions, whereas the addition of a fourth dimension brought little further improvement. As expected, the first two dimensions lent themselves for interpretation as perceptual colour-opponent systems, R/G and B/Y. The third dimension was interpretable as variation of lightness (Value) among stimuli.

Each solution can be written as a 30-by-3 matrix **X**, where the *i*-th row contains the coordinates $\{x_{i1}, x_{i2}, x_{i3}\}$ that locate that hue along the three dimensions of the colour space. Sometimes a MDS solution can be rotated to bring its axes into correspondence with the familiar colour dimensions, so that the contribution from two points' separation along the first axis (i.e. x_{i1}-x_{j1}) corresponds to their displacement along (e.g.) the R/G dimension, and so on. This cannot be assumed in advance, however.

When the three group exploratory solutions were compared (as detailed below), they gave the impression that subjects in the clinical groups tended to be less sensitive to blue-yellow colour differences, resulting in a compression of colour space along the corresponding axis, but only for the *desaturated* hues. This impression was quantified in a confirmatory stage, analysing each subject's data in isolation.

Confirmatory analysis

Our previous research with the same method and hues and a larger pool of subjects (Ref. 12, Figure 1) provided $\mathbf{X}_0$, a 'standard' matrix of coordinates in a default, consensus colour space. In the present analysis, $\mathbf{X}_0$ was distorted (compressed) to produce individual colour spaces $\mathbf{X}_m$

tailored to the *m*-th subject's responses. This entailed two subject-specific parameters, w_{m2} and w_{m3} (or two parameters for each *eye* of subjects in the clinical populations).

For each individual space $\mathbf{X}_m$, w_{m2} is the weight or salience of the second dimension relative to the first dimension: $x_{mi2} = w_{m2}\, x_{0i2}$ (where the index *i* labels the hues). Because $\mathbf{X}_0$ has been rotated so that its second dimension corresponds to the tritan confusion axis, values of $w_{m2} < 1$ indicate blue-yellow (tritan) deficiency, ranging in severity, with its extreme form, tritanopia, indicated by $w_{m2} = 0$ (i.e. subject *m* would see no distinction between two hues that differ only in stimulation to the S-cones, and are separated only along the B/Y axis). Conversely, $w_{m2} > 1$ results if the *m*-th subject is relatively insensitive to red-green differences, with larger values indicating increasingly severe R/G deficiency.

So far we follow a number of precedents. However, in a departure from that research tradition, the model tested here only imposes w_{m2} upon the locations of the *desaturated* hues – with the *saturated* hues retaining their default values of x_{0i2} – based on the evidence that any acquired colour deficiency disproportionately affects discrimination of desaturated colours.

Recall that the desaturated D-15d caps differ from those of the D-15 series in lightness (Value). Combined with the range of hues, the lightness differences require a third dimension to accommodate them within the solutions from the exploratory analyses. $\mathbf{X}_0$ is likewise three-dimensional, with the D-15 and D-15d points occupying two parallel planes. Notably, subjects can vary in the weight they place on lightness differences in their dissimilarity perceptions.[49,50] The parameter w_{m3} accommodates these variations through the equation $x_{mi3} = w_{m3}\, x_{0i3}$.

The two parameters, w_{m2} and w_{m3}, were adjusted systematically, summing $LL(\mathbf{X}_m)$ for each combination, to find the particular values that maximized the fit between $\mathbf{X}_m$ and the *m*-th data set. The distributions of w_{m2} and w_{m3} within each subject group can be compared among the control and two clinical groups, and any differences tested for significance.

Results

MDS analysis

We examined two-dimensional and three-dimensional MDS solutions for each subject group. In each case the third dimension was interpretable (after rotation) as lightness or Value, arranging the points in two roughly parallel planes in space. To reduce the degrees of freedom and for ease of display, we also examined constrained solutions in which the darker D-15 caps (V = 5) all shared a single coordinate on the third dimension (i.e. the mean around which they cluster), and the lighter D-15d caps (V = 8) all shared a second common coordinate.

The log-likelihoods for 2D solutions for the controls, Hg and DM-2 groups were $LL(\mathbf{X})$ = -848, -2420 and -3650 respectively. For constrained 3D solutions with one additional degree of freedom the corresponding values were -794, -2070 and -3380, the improvements being ΔLL = 54, 350 and 270. According to the Likelihood Ratio Test, $2\Delta LL$ follows a χ^2 distribution, so the improvements are all significant ($p < 0.001$).[46] Unconstrained 3D solutions (with another 26 degrees of freedom) bring $LL(\mathbf{X})$ up to -753, -1990 and -3295. Though smaller, the further improvements ΔLL = 41, 80 and 85 are all significant, i.e. the third-dimensional coordinates do depart from the two parallel planes.

Figure 1 shows the constrained 3D solutions, labelled for convenience $\mathbf{X}_{C}$ (controls), $\mathbf{X}_{Hg}$ and $\mathbf{X}_{DM\text{-}2}$. Oblique perspectives are shown in the left-hand panels. The right-hand panels show projections on the first two dimensions, which can be interpreted as Red-Green ($D1$) and Blue-Yellow ($D2$) gradients. Consistently, the saturated and desaturated colours are each arranged in a rough horseshoe (shown by solid and dotted lines respectively), following the expected sequence from Purple (5P) through Red (5R), Yellow (5Y) and Green (5G) through to Blue (5B). The 15 stimuli comprising the ‘composite assortment’ are localised more tightly than the other 15, because (as noted in the Procedure) they were triangulated by appearing in 13 times as

many triads. The stimuli *excluded* from the assortment are localised in the top, middle and bottom panels of Figure 1 by 23, 44 and 66 triads respectively, and their confidence bounds would be looser.

Figure 1 about here

The constrained MDS confines the stimulus-points to two planes – separated by the third dimension, lightness, or Value (*D*3) – as shown in the left-hand panels. These planes contain respectively the darker/saturated stimuli (Value = 5, Chroma = 4) and the lighter/desaturated stimuli (Value = 8, Chroma = 2).

The right-hand panel for control normal trichromats ($\mathbf{X}_C$) shows the two stimulus sequences spanning similar ranges of the first two dimensions. That is, corresponding dissimilarities among saturated and desaturated colours are seen as comparable, even though the former are twice as far from White as the latter in Munsell terms (Chroma = 4 vs. 2) or greater in CIE1931 terms (see Ref. 5, Figure 2). This is not unexpected, since in earlier results other groups of normal trichromats were equally willing to discount saturation [8,11].

There is a crucial contrast in the two clinical population solutions, $\mathbf{X}_{Hg}$ and $\mathbf{X}_{DM\text{-}2}$. There, both sequences are spread out equally along the R/G axis but the desaturated stimuli do not seem to occupy as much of the B/Y axis as do the saturated stimuli. That is, the arrangement of desaturated stimuli is elliptical rather than circular. In addition the gap separating the desaturated stimuli from saturated stimuli along the lightness dimension *D*3 appears to be larger (left-hand panels).

These visual impressions can be tested by examining the dispersal of points along each axis of the MDS solution (i.e. the variance of coordinates along each axis), as a fraction of total variance (Table 1). *D*1 disperses the stimuli by about the same extent in all three solutions. However, compared to the controls, the dispersal for the clinical groups is smaller along *D*2 (Blue-Yellow), with a compensatory increase along *D*3 (Value). More specifically, when we

partition the *D*2 dispersal into separate contributions from the saturated and desaturated stimuli, the decrease in the two clinical groups is confined to the desaturated component.

Table 1 about here

Note that this kind of saturation-dependent effect does not conform to the assumptions of the weighted-Euclidean model of individual differences. Inter-subject variations of this form can be modelled within the weighted-Euclidean framework, but the resulting dimensional-salience parameters will be a compromise between saturated and desaturated stimulus sets.

Confirmatory analysis

To disentangle the dissimilarity impact on saturated and desaturated colours, individual subjects' responses were fitted separately for a model of individual variation suggested by Figure 1, in which a parameter w_{m2} tailors a standard colour space $\mathbf{X}_0$ by varying the B/Y contribution to inter-item dissimilarity, but only for the desaturated stimuli. A second parameter w_{m3} reflects the dissimilarity contribution from lightness differences. The distributions of the parameters are plotted as histograms for each group in Figure 2. Values of w_{m2} were lower across the clinical groups compared to the controls ($p = 0.004$), to the extent that many subjects appeared to be oblivious to the blueness or yellowness of desaturated stimuli. The group differences remained significant when comparing controls to the DM-2 group, but not to the Hg group separately (Table 2); the two clinical groups did not differ significantly.

Figure 2, Table 2 about here

When presented with triads that comprised one (or two) lighter/less saturated stimuli and two (or one) darker/saturated stimuli, the Hg and DM-2 subjects also attended more than the controls to lightness when choosing the odd-one-out, as reflected in higher w_{m3} values (Figure

2, bottom). The difference in the w_{m3} distributions was significant between the control and both clinical groups (Table 2), with no significant difference between the clinical groups.

Figure 3 plots w_{m3} against w_{m2}, with the three subject groups distinguished by colour. Points for seven representative subjects are plotted in the w_{m2} / w_{m3} 'weight plane' in Figure 4, with confidence bounds. In each case the ellipsoidal outer bound is the locus of weights where the Likelihood of the weighted $\mathbf{X}_m$ predicting the observed responses falls to 0.01 of its maximised value [i.e. $LL(\mathbf{X}_m)$ is lower by log(0.01) = -4.6], while the Likelihood at the inner bound is 0.05 of its maximised value [$LL(\mathbf{X}_m)$ is lower by -3].

Figures 3, 4 about here

Finally, we found that likelihood was significantly lower across each of the two clinical groups than across the control group (Table 2). This is consistent with global difficulty in colour discrimination in addition to the blue-yellow deficiency apparent here. Likelihoods would also be lower if our model of individual differences simply was not valid for the Hg and DM-2 groups; i.e. these subjects' responses could be highly discriminant, and consistent with colour spaces derived from $\mathbf{X}_0$, but through some other transformation. However, this interpretation is not compatible with Figure 1.

As an afterthought we applied a more conventional Weighted Euclidean model of individual variation, varying the parameters w_{m2} and w_{m3}, but applying the former to all stimuli (saturated as well as desaturated). Mean values for w_{m2} did not differ so much between groups: 0.98, 0.91 and 0.90, for the controls, Hg and DM-2 respectively. The difference between w_{m2} values for the controls and the combined clinical groups no longer quite reached significance (p = 0.063). However, mean likelihood values were lower for this model than for the desaturation-specific model, causing us to prefer the latter.

Discussion

Previous MDS analyses of these data[14,15] considered each observer's responses separately, and focussed on the five D15 and ten D-15d caps used in the combined assortment, omitting the other 15 caps that each observer only sorted once. Even so, the sparse nature of the data limited them to two-dimensional solutions. In contrast, the Exploratory phase of the present analysis could sustain three-dimensional solutions because responses were pooled for each group. This in turn enabled us to observe differences in dimensional-salience parameters.

The D-15 and D-15d tests of colour vision deficiency use colour samples that are spaced at roughly equal intervals around the hue circle and, within each test, do not vary in lightness or saturation. As normally administered, they do not probe the salience of lightness differences to a subject or test for saturation-dependent impairments. Combining the sample sets, as in the present study, introduces variations along these two achromatic characteristics (cf. Ref. 51).

The results suggest that in the two clinical groups, the signal along the S_0 or tritan system is greatly decreased for a stimulus containing a small component of blueness or yellowness, leaving the redness or greenness of the stimulus to dominate stimulus appearance and distorting its dissimilarities from other stimuli. Thus in the MDS solution, the desaturated stimuli collapse towards the R/G axis. Conversely, the dissimilarities perceived among the saturated stimuli are comparable to those for the controls, implying that sufficiently large blue or yellow components can still be detected and produce a normal S_0 signal.

A possible explanation is that mercury exposure and DM-2 impair the detection sensitivity of the S_0 mechanism of colour vision. Blue-yellow sensitivity loss has indeed been reported in the case of mercury intoxication.[21,23] The decreased S_0 sensitivity is conceivably followed by a compensatory amplification along the blue-yellow system, but only if the original signal is large enough to rise above the threshold of noise.[16]

Köllner's rule states that an acquired blue-yellow deficiency can be traced to damage to the retina.[52] Note though that mercury can affect the visual system in numerous ways, also impacting on the optic nerve and visual cortex.[26,27]

One cannot expect either of the clinical groups to be homogeneous, given the large variations in the factors contributing to their acquired colour vision deficiency, i.e. length and dosage of mercury exposure and the progressive nature of DM-2. Indeed, the MDS approach reveals considerable variation in the Hg-exposed and DM-2 groups: despite their tendency *as groups* toward lower w_{m2}, some fell within the distribution of control observers and some departed from the controls in the opposite direction, towards insensitivity to red-green differences (Figures 2 and 3). Thus estimating the weights of colour-space axes is not on its own sufficient to unambiguously diagnose the stage of diabetes progression or the impact of mercury exposure. However, the tendency is a reminder of the importance of examining colour vision function when either condition is suspected.

Several studies of mercury-exposed populations that used the Cambridge Colour Test to quantify chromatic discrimination thresholds directly along protan, deutan and tritan confusion lines[24,25,28,32] all found a general, diffuse loss of sensitivity, rather than increased thresholds confined to a specific axis. Note though that in these studies the threshold measurements were averaged across subjects – who were affected to various degrees and may have suffered from different forms of colour vision deficiency.

Clinical group subjects were tested twice, with left and right eye. The correlations between calculated left-eye and right-eye parameters are significant (at $p = 0.003$ or less): 0.391 for w_{m2}, 0.558 for w_{m3}, and 0.566 for likelihood l_m. Some of the differences may be real, since visual impairment from mercury exposure or diabetes need not affect both eyes with equal severity.[29] However, the confidence bounds around these dimensional weights (Figure 4) indicate that 70 triads are not enough to confine their values very closely, reducing the test–retest reliability of the MDS analysis.

The higher mean w_{m3} in the two clinical groups may indicate a form of compensation for less reliable chromatic discrimination, with these subjects placing more weight on lightness cues as a criterion for making odd-one-out judgements. The high correlation between w_{m3} for left-eye and right-eye observations suggests that the increase is central rather than peripheral in nature, e.g. binocular interaction and/or attentional factors. Notably, Stalmeier and de Weert, using the complete method of triads, found that the salience of lightness was modulated by selective attention.[53] Increased weight of the lightness dimension was also found for congenitally colour abnormal observers.[49, 50,54]

This 'compensatory' explanation leaves open a second possibility: the fact is that w_{m3} is not measured in absolute terms, but only relative to the weight placed on the first, R/G dimension; hence any condition that impairs red-green discrimination without affecting lightness discrimination necessarily increases the *relative* weight of the latter.

Finally, the significantly lower likelihoods l_m for colour spaces of subjects in the clinical groups (Table 2) deserve further comment. Specifically, if the affected subjects viewed colour differences in the distorted way modelled here, i.e. decreased distances along the Blue-Yellow axis for desaturated stimuli, but made odd-one-out judgements that were reliable in those distorted terms, their l_m values would be no lower than those of the controls. The observed low values of l_m indicate that clinical group subjects were in fact responding less reliably, i.e. their colour discrimination was generally poorer.

The present approach may be sensitive to conditions such as complex dyschromatopsia, which the conventional D-15d appears to underestimate.[55] The analysis is equally applicable to data elicited with other tasks, for instance pairwise numerical scaling. The method of triads has advantages, though, including the relative simplicity of the judgments required of the subject,[56] and the simplicity of Maximum Likelihood estimation when the data take the form of dissimilarity comparisons.[46] The use of randomized triads rather than a standardized list introduces some variation among subjects. Future research in this direction could use a

standard, pre-determined list of triads; for instance, a ‘balanced incomplete design’ with $\lambda = 2$ where each pair of stimuli appears twice.[56]

We have noted that MLE provides an objective test for choosing between alternative explanatory models, the Likelihood Ratio test. This is suitable for comparing *nested* models where one model’s parameters are a subset of the other’s. Another test, the Akaike Information Criterion (AIC), is available for comparing Likelihood values between non-nested models.[46] A further advantage of the MLE approach is the ease with which confidence bounds can be found around parameters when fitting models to individuals or groups to summarise their data.

The resulting data can capture subtle but distinctive patterns of colour-vision impairment when analysed with individual-differences MDS. There are potential applications as a diagnostic tool – assuming that more triads are collected – and for monitoring the status of an acquired condition. A mixed stimulus set was used, with two values of lightness and saturation, because the dimensions of colour space spanned by the stimuli define the forms of impairment and compensation detectable in this way. A realistic model of individual difference is a second requirement. The model introduced here – that posits impaired discrimination restricted to unsaturated colours – is more in keeping with clinical reports than the usual weighted-Euclidean model, and appears to be a better fit to the data.

Appendix: Maximum-Likelihood Estimation MDS

When a subject chooses cap A as the odd-one-out of the triad {A,B,C}, this is tantamount to ranking the cap pair (B,C) as more similar than the two other pairs (A,B) and (A,C). Writing 'diss(A,B)' for the subjective dissimilarity between A and B, this in turn can be considered as a pair of dissimilarity comparisons: diss(A,B) > diss(B,C), diss(A,C) > diss(B,C), at the time of the decision. It is convenient to express this in a shorthand form: AB » BC, AC » BC.

MDS postulates that diss(A,B) can be modelled by the distance d_{AB} in a low-dimensional space. Specifically, we assume without loss of generality that diss(A,B) = d_{AB} + $e(0)$, where $e(0)$ is a random error term with a mean of 0. If the subject were infallible, so $e(0) = 0$, his or her choices would follow a step probability function of the difference between distances $\Delta(AB,BC) = d_{AB}-d_{BC}$:

$$\text{pr}(AB \text{ » } BC) = \begin{cases} 1 \text{ if } \Delta(AB,BC) > 0 \\ 0.5 \text{ if } \Delta(AB,BC) = 0 \\ 0 \text{ if } \Delta(AB,BC) < 0. \end{cases}$$

In practice, of course, subjects are fallible – or rather, they are inconsistent, with the perception of any dissimilarity changing from one comparison to another – and although the probability approaches 0 or 1 if $\Delta(AB,BC)$ is sufficiently negative or positive, the transition between them is a smooth ogive. Following Thurstone's Model of Pairwise Comparison, we assume that the error contributions are normal in form. Then $\text{pr}(AB \text{ » } BC \mid \Delta(AB,BC)) = \Phi(\beta \Delta(AB,BC))$, where the cumulative density function $\Phi(x)$ is the integral of the normal distribution and the parameter β is the observer's 'discriminance', higher values denoting a more discerning, consistent set of judgements.

The likelihood that a given combination of interpoint distances in a spatial model would have produced the observed list of dissimilarity comparisons from a given subject – or from a *group* of subjects being analysed together – is the *product* of all the corresponding probabilities. In the present case there are 140 comparisons per subject (two from each triad), ranking the 435 dissimilarities among the 30 stimuli. Their product is a goodness-of-fit function, with

Maximum Likelihood Estimation working to maximise this combined likelihood by finding the optimum values of parameters.

It is convenient to work with the logarithm of the likelihood, so as to replace the product with a sum of terms:

LL = log likelihood = Σ log($\Phi(\beta\ \Delta(\mathrm{AB,BC}))$).

A version of this, normalised over the subject's 140 comparisons, is $l_m = \exp(LL/140)$.

For comparison, the older MDS programs MINITRI[57] and TRISOSCAL[58] employ a least-squares algorithm that defines and minimises a 'badness-of-fit' *Stress* function. Each comparison of the form AB » BC contributes a quadratic term $(d_{\mathrm{AB}}\text{-}d_{\mathrm{BC}})^2$ to *Stress* if $d_{\mathrm{AB}} < d_{\mathrm{BC}}$, or 0 if the model agrees with the data ($d_{\mathrm{AB}} > d_{\mathrm{BC}}$). It is worth noting that for sufficiently large discriminance β, the MLE and least-squares algorithms become equivalent (i.e. the former includes the latter as a special case), due to the nature of the $\log(\Phi(x))$ function, which becomes quadratic for large negative values of x while levelling off at 0 for large positive x.

In one of the present analyses, the parameters are the coordinates x_{ip} locating 30 points in three-dimensional space ($1 \le i \le 30$, $1 \le p \le 3$), which can be written as a 30-by-3 matrix **X**. MTRIAD follows a hill-climbing strategy. The coordinates are optimised through a series of iterations **X**, **X**', **X**"..., in a process analogous to the two-dimensional case of climbing a hill, by finding the direction at each **X**' in which the slope is steepest (i.e. in which $LL(\mathbf{X})$ increases most rapidly) and taking a step in that direction.

For this, the partial differential of Likelihood for each inter-point distance $\partial LL(\mathbf{X})/\partial d_{ij}$ is calculated: for every comparison in the data between that pair of stimuli and another pair, there is a contribution of the form $\partial\log(\Phi(\beta\ (d_{ij}\text{-}d_{jk}))) / \partial d_{ij}$. These differentials $\partial LL(\mathbf{X})/\partial d_{ij}$ are converted into partial differentials for each *coordinate*, $\partial LL(\mathbf{X})/\partial x_{ip}$. The hill-climbing strategy is also common in least-squares implementations of MDS, though the individual contributions are simpler. Constraints among the coordinates are easily incorporated in this process.

References

1. Farnsworth D. Farnsworth-Munsell 100-Hue and Dichotomous test for color vision. J. Opt. Soc. Am. 1943; 33: 568–578.

2. Lanthony P. The Desaturated Panel D-15. Doc. Ophthalmol. 1978; 46: 185-189.

3. Birch J. Diagnosis of defective colour vision. Oxford: Oxford University Press; 1993.

4. Dain SJ. Clinical colour vision tests. Clin. Exp. Optom. 2004; 4:276–293.

5. Geller AM, Hudnell HK. Critical issues in the use and analysis of the Lanthony Desaturate Color Vision Test. Neurotoxicol. Teratol. 1997; 19:455-465.

6. Paramei GV, Meyer-Baron M, Seeber A. Impairments of colour vision induced by organic solvents: a meta-analysis study. NeuroToxicology 2004; 25:803-816.

7. Bimler D, Kirkland J, Jacobs R. Colour-vision tests considered as a special case of multidimensional scaling. Color Res. Appl. 2000; 25:160-169.

8. Bimler DL, Kirkland J, Jameson KA. Quantifying variations in personal color spaces: Are there sex differences in color vision? Color Res. Appl. 2004; 29:128-134.

9. Torgerson WS. Multidimensional scaling: I. Theory and method. Psychometrika 1952; 17: 401-419.

10. Helm CR. Multidimensional ratio scaling analysis of perceived color relations. J. Opt. Soc. Am. 1964; 54:256-262.

11. Bimler D, Kirkland J. Multidimensional scaling of D15 caps: Color-vision defects among tobacco smokers? Vis. Neurosci. 2004; 21:445-448.

12. Bimler D, Kirkland J. Quantifying color-space variations with a triadic procedure: A twin study of genetic contributions to color vision. Clin. Exp. Optom. 2004; 87:313-321.

13. Bimler D, Kirkland J. Colour-space distortion in women who are heterozygous for colour deficiency. Vision Res. 2009; 49:536–543.

14. Feitosa-Santana C, Bimler DL, Paramei GV, Oiwa NN, Barboni MTS, Costa MF, Silveira LCL, Ventura DF. Color-space distortions following long-term occupational exposure to

mercury vapor. Ophthalmic & Physiol. Opt. 2010; 30:724–730.

15. Feitosa-Santana C, Oiwa NN, Paramei GV, Bimler D, Costa MF, Lago M, Nishi M, Ventura DF. Color space distortions in patients with type 2 diabetes mellitus. Vis. Neurosci. 2006; 23:663-668.

16. Krastel H, Moreland JD. Colour vision deficiencies in ophthalmic diseases. In Foster DH, editor. Inherited and acquired colour vision deficiencies. London: Macmillan; 1991. p. 115-172.

17. Bakir F, Damluji SF, Amin-Zaki L. Methylmercury poisoning in Iraq. Science 1973; 181:230-241.

18. Lebel J, Mergler D, Lucotte M, Amorim M, Dolbec J, Miranda D, Arantès G, Rheault I, Pichet P. Evidence of early nervous system dysfunction in Amazonian populations exposed to low-levels of methylmercury. NeuroToxicology 1996; 17:157-168.

19. Lebel J, Mergler D, Branches F, Lucotte M, Amorim M, Larribe F, Dolbec J. Neurotoxic effects of low-level methylmercury contamination in the Amazonian Basin. Environ. Res. 1998; 79:20–32.

20. Meyer-Baron M, Schaeper M, Seeber A. A meta-analysis for neurobehavioral results due to occupational mercury exposure. Arch. Toxicol. 2002; 76:127-136.

21. Cavalleri A, Belotti L, Gobba FM, Luzzana G, Rosa P, Seghizzi P. Colour vision loss in workers exposed to elemental mercury vapour. Toxicol. Lett. 1995; 77:351-356.

22. Cavalleri A, Gobba FM. Reversible color vision loss in occupational exposure to metallic mercury. Environ. Res. 1998; 77:173-177.

23. Urban P, Gobba F, Nerudová J, Lukáš E, Čábelková Z, Cikrt M. Color discrimination impairment in workers exposed to mercury vapor. NeuroToxicology 2003; 24:711-716.

24. Silveira LCL, Damin ETB, Pinheiro MCN, Rodrigues AR, Moura ALA, Cortes MIT, Mello GA. Visual dysfunction following mercury exposure by breathing mercury vapour or by eating mercury-contaminated food. In Mollon JD, Pokorny J, Knoblauch K editors.

Normal and defective colour vision. Oxford: Oxford University Press; 2003. p. 407–417.

25. Ventura DF, Costa MTV, Costa MF, Berezovsky A, Salomão SR, Simões AL, Lago M, Pereira LHMC, Faria MAM, De Souza JM, Silveira LCL. Multifocal and full-field electroretinogram changes associated with color-vision loss in mercury vapor exposure. Vis. Neurosci. 2004; 21:421–429.

26. Pokorny J, Smith VC, Verriest G, Pinckers AJLG. Congenital and acquired color defects. New York, NY: Grune & Stratton; 1979.

27. Korogi Y, Takahashi M, Hirai T, Ikushima I, Kitajima M, Sugahara T, Shigematsu Y, Okajima T, Mukuno K. Representation of the visual field in the striate cortex: comparison of MR findings with visual field deficits in organic mercury poisoning (Minamata disease). Am. J. Neuroradiol. 1997; 18:1127-1130.

28. Ventura DF, Simões AL, Tomaz S, Costa MF, Lago M, Costa MTV, Canto-Pereira LHM, de Souza, JM, Faria MAM, Silveira LCL. Colour vision and contrast sensitivity losses of mercury intoxicated industry workers in Brazil. Environ. Toxicol. Pharmacol. 2005; 19:523–529.

29. Verriest G. Les déficiences acquises de la discrimination chromatique. Bulletin et Mémoire de L'Académie Royale de Médecine de Belgique 1964; II/IV/5:35-327.

30. Mollon JD, Reffin JP. Handbook of the Cambridge Colour Test. London (UK): Cambridge Research Systems; 2000. http://visl.technion.ac.il/projects/2002w/theory.pdf

31. Feitosa-Santana C, Barboni MTS, Oiwa NN, Paramei GV, Simões AL, Costa MF, Silveira LCL, Ventura DF. Irreversible color vision losses in patients with chronic mercury vapor intoxication. Vis. Neurosci. 2008; 25:487–491.

32. Canto-Pereira LHM, Lago M, Costa MF, Rodrigues AR, Saito C, Silveira LCL, Ventura DF. Visual impairment on dentists related to occupational mercury exposure. Environ. Toxicol. Pharmacol. 2005; 19:517–522.

33. Ismail GM, Whitaker D. Early detection of changes in visual function in diabetes mellitus.

Ophthalmic Physiol. Opt. 1998; 18:3-12.

34. Kurtenbach A, Mayser HM, Jägle H, Fritsche A, Zrenner E. Hyperoxia, hyperglycemia, and photoreceptor sensitivity in normal and diabetic subjects. Vis. Neurosci. 2006; 23:651-661.

35. Lakowski R, Aspinall PA, Kinnear PR. Association between colour vision losses and diabetes mellitus. Ophthalmic Res. 1972/1973; 4:145-159.

36. Roy MS, Gunkel RD, Podgor MJ. Color vision defects in early diabetic retinopathy. Arch. Ophthalmol. 1986; 104:225-228.

37. Utku D, Atmaca LS. Farnsworth-Munsell 100-hue test for patients with diabetes mellitus. Ann. Ophthalmol. 1992; 24:205-208.

38. Feitosa-Santana C, Paramei GV, Costa MF, Gualtieri M, Nishi M, Ventura DF. Color discrimination in type 2 diabetes assessed by the D-15d test and the Cambridge Colour Test. Ophthalmic Physiol. Opt. 2010; 30:717-723.

39. Kurtenbach A, Flögel W, Erb C. Anomaloscope matches in patients with diabetes mellitus. Graefes Arch. Clin. Exp. Ophthalmol. 2002; 240:79-84.

40. Trick GL, Burde RM, Gordon MO, Santiago JV, Kilo C. The relationship between hue discrimination and contrast sensitivity deficits in patients with diabetes mellitus. Ophthalmol. 1988 ; 95:693-698.

41. Ventura DF, Costa MF, Gualtieri M, Nishi M, Bernick M, Bonci D, de Souza JM. Early vision loss in diabetic patients assessed by the Cambridge Colour Test. In Mollon JD, Pokorny J, Knoblauch K editors. Normal and defective colour vision. Oxford: Oxford University Press; 2003. p. 395-403.

42. Barton FB, Fong DS, Knatterud GL, ETDRS Research Group. Classification of Farnsworth-Munsell 100-Hue Test results in the Early Treatment Diabetic Retinopathy Study. Am. J. Ophthalmol. 2004; 138:119-124.

43. Bresnick GH, Condit RS, Palta M, Korth K, Groo A, Syrjala S. Association of hue discrimination loss and diabetic retinopathy. Arch. Ophthalmol. 1985;103:1317-1324.

44. Fong DS, Barton FB, Bresnick GH. Impaired color vision associated with diabetic retinopathy: Early Treatment Diabetic Retinopathy Study Report No. 15. Am. J. Ophthalmol. 1999; 128:612-617.

45. Smith VC, Van Everdingen JAM, Pokorny J. Sensitivity of arrangement tests as evaluated in normals at reduced levels of illumination. In: Drum B, Moreland JD, Serra A editors. Colour vision deficiencies X. Documenta Ophthalmologica. Proceedings, Series 54. Dordrecht: Kluwer; 1991. p. 177–185.

46. Takane Y. A maximum likelihood method for nonmetric multidimensional scaling: I. The case in which all empirical pairwise orderings are independent – Theory. Jap. Psych. Res. 1978; 20:7-17.

47. Knoblauch K, Maloney LT. MLDS: Maximum likelihood difference scaling in R. J. Stat. Software 2008; 25:1–26.

48. Maloney LT, Yang JN. Maximum likelihood difference scaling. J. Vision 2003; 3:573-585.

49. Paramei GV, Bimler D. Vector coding underlying individual transformations of a color space. In: Musio C editor. Vision: The approach of biophysics and neurosciences: Series on Biophysics and Biocybernetics, Vol. 11. Singapore: World Scientific; 2003. p. 429-436.

50. Paramei GV, Bimler DL. Is color space curved? A common model for color-normal and color-deficient observers. In: Backhaus W editor. Neuronal coding of perceptual systems: Series on Biophysics and Biocybernetics, Vol. 9. Singapore: World Scientific; 2003. p. 102-105

51. Indow T, Kanazawa K. Multidimensional mapping of Munsell colors varying in hue, chroma, and value. J. Exp. Psych. 1960; 59:330-336.

52. Köllner H. Die Störungen des Farbensinnes. Ihre klinische Bedeutung und ihre Diagnose.

Berlin: Karger; 1912.

53. Stalmeier PFM, de Weert CMM. Large color differences and selective attention. J. Opt. Soc. Am. A 1991; 8:237-247.

54. Paramei GV, Bimler D, Cavonius CR. Color-vision variations represented in an individual-difference vector chart. Color Res. Appl. 2001: 26 (Supplement): S230-S234.

55. Mergler D, Blain L. Assessing color vision loss among solvent-exposed workers. Am. J. Ind. Med. 1987; 12:195-203.

56. Burton ML, Nerlove SB. Balanced designs for triads tests: Two examples from English. Soc. Sci. Res. 1976; 5:247–267.

57. Roskam EE. The method of triads for nonmetric multidimensional scaling. Ned. Tijdschr. Psychol. 1970; 25:404-417.

58. Coxon APM, Jones CL. The images of occupational prestige. London: Macmillan; 1978.

Acknowledgements

Supported by FAPESP, CNPq, CAPES/PROCAD, FINEP IBN-Net. DFV is a CNPq fellow; CFS and NNO were FAPESP fellows.

Table legends

Table 1. Variance of the coordinates along each dimension of colour space (as a fraction of total variance in that solution) for MDS solutions of the controls ($\mathbf{X}_{C}$), mercury-exposed subjects ($\mathbf{X}_{Hg}$) and diabetes patients ($\mathbf{X}_{DM\text{-}2}$).

Table 2. Means and standard errors for dimension-weight parameters w_{m2}, w_{m3} and normalised likelihood-per comparison $l_m = \exp(LL(\mathbf{X}_m)/140)$ within each group, when $\mathbf{X}_0$ is adjusted to each subject's responses (left-hand columns). Probability (*t*-value) of pairwise differences between the groups (right-hand columns). These dimensional parameters are not measured in absolute terms, only relative to $w_{m1} = 1$ for all observers.

Figure legends

Figure 1. The three-dimensional MDS solutions for triadic data from controls (top), mercury (Hg)-exposed subjects (middle), and diabetes (DM-2) patients (bottom). Perspective views (left) and projections on the first two dimensions (right). –– darker/saturated D-15 caps; ···· lighter/desaturated D-15d caps. The labels of caps along the desaturated sequence in right-hand panels are omitted for the sake of clarity.

Figure 2. Distributions of dimensional-weight parameters fitted to data from individual subjects in the three groups (controls, Hg-exposed and DM-2 patients): w_{m2}, salience of differences along the Blue-Yellow dimension, $D2$ (top), and w_{m3}, salience of differences along the lightness dimension, $D3$ (bottom).

Figure 3. Scatterplot of dimensional-weight parameters w_{m2} and w_{m3} fitted to individual subjects' data. Points colour-coded to distinguish controls, mercury (Hg)-exposed subjects and diabetes (DM-2) patients.

Figure 4. Parameters w_{m2} and w_{m3} for seven representative subjects (two from Control, two from Hg and three from DM-2 groups, points coloured as in Figure 3), each surrounded by 95% and 99% confidence boundaries (darker and lighter ellipsoids).

Table 1

	$D1$	$D2$ =	$D2$ (sat.)+$D2$ (desat.)		$D3$
$\mathbf{X}_{C}$	0.54	0.28	0.16	0.12	0.16
$\mathbf{X}_{Hg}$	0.48	0.22	0.14	0.08	0.29
$\mathbf{X}_{DM\text{-}2}$	0.53	0.23	0.15	0.07	0.25

Table 2

	controls	Hg	DM-2	C : clinical 131 d.f.	C : Hg 65 d.f.	C : DM-2 87 d.f.
		mean (SE)			p (t)	
w_{m2}	1.08 (0.07)	0.91 (0.09)	0.76 (0.06)	0.004 (3.04)	n.s. (1.52)	0.001 (3.53)
w_{m3}	1.02 (0.10)	1.56 (0.08)	1.41 (0.06)	0.000 (-4.39)	0.000 (-4.30)	0.000 (-3.80)
l_m	0.734 (0.024)	0.644 (0.018)	0.623 (0.021)	0.003 (3.05)	0.005 (2.94)	0.005 (2.91)

Figure 1

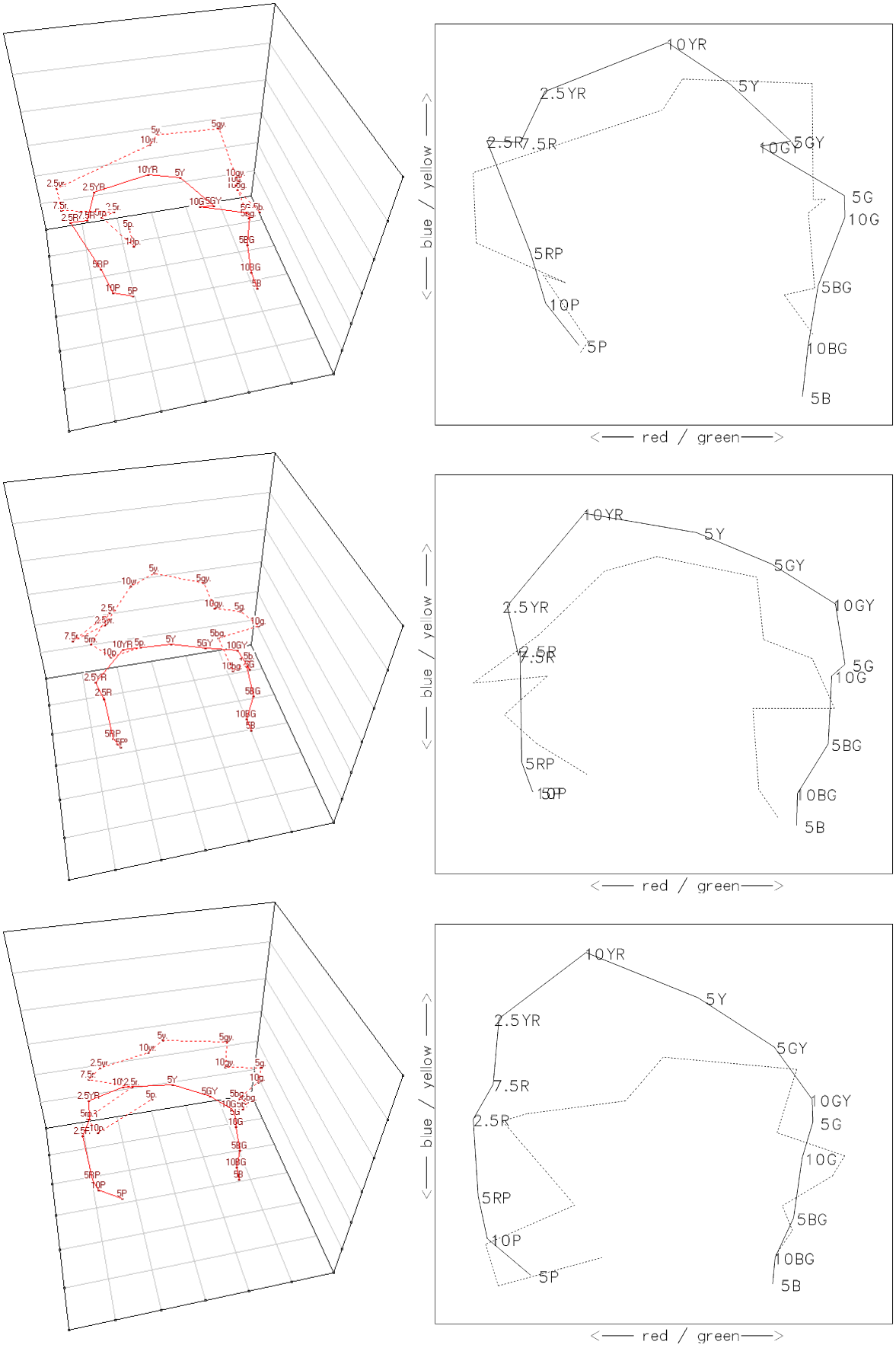
10YR
2.5YR
5Y
2.5R
7.5R
10GY
5GY
5G
10G
5RP
5BG
10P
5P
10BG
5B
< blue / yellow >
< red / green >
10YR
5Y
5GY
2.5YR
10GY
2.5R
7.5R
5G
10G
5BG
5RP
10P
10BG
5B
< blue / yellow >
< red / green >
10YR
5Y
2.5YR
5GY
7.5R
10GY
2.5R
5G
10G
5RP
5BG
10P
10BG
5P
5B
< blue / yellow >
< red / green >

Figure 2

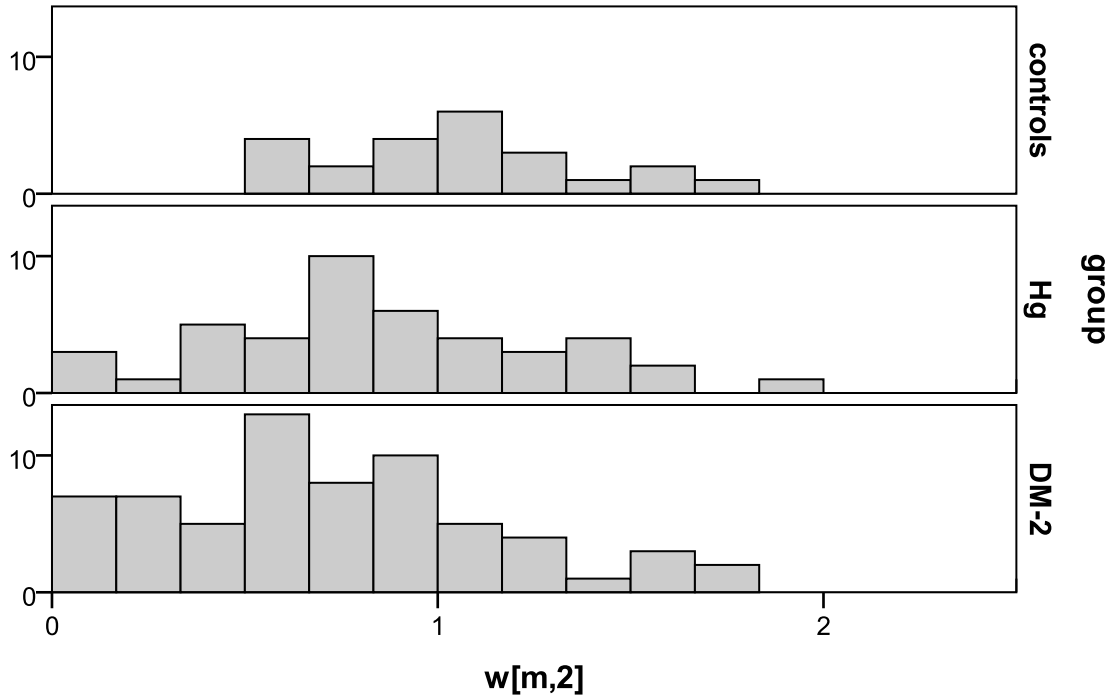
10
0
controls
10
0
Hg
10
0
DM-2
group
0
1
2
w[m,2]

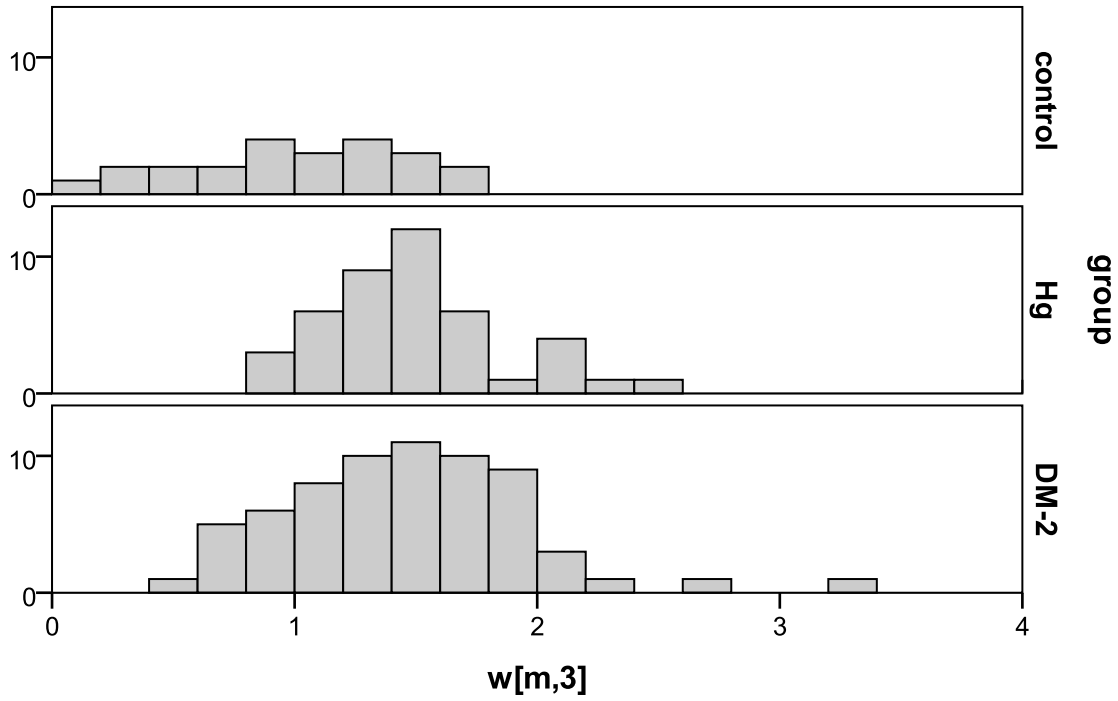
10
0
control
10
0
Hg
10
0
DM-2
group
0
1
2
3
4
w[m,3]

Figure 3

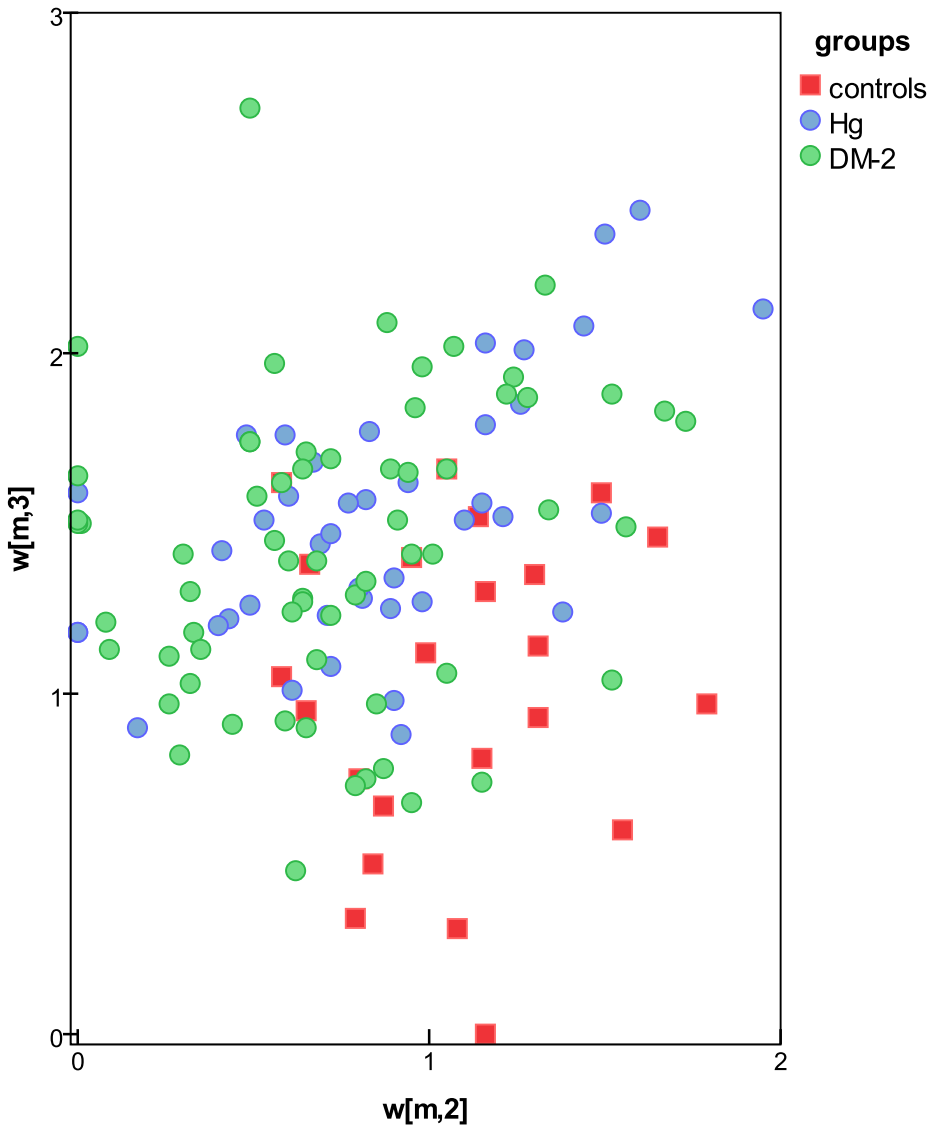

Figure 4